Oblique frozen modes in periodic layered media

A. Figotin and I. Vitebskiy
Department of Mathematics, University of California, Irvine, Irvine, California 92697, USA
(Received 9 April 2003; revised manuscript received 27 May 2003; published 17 September 2003)

We study the classical scattering problem of a plane electromagnetic wave incident on the surface of semi-infinite periodic stratified media incorporating anisotropic dielectric layers with special oblique orientation of the anisotropy axes. We demonstrate that an obliquely incident light, upon entering the periodic slab, gets converted into an abnormal grazing mode with huge amplitude and zero normal component of the group velocity. This mode cannot be represented as a superposition of extended and evanescent contributions. Instead, it is related to a general (non-Bloch) Floquet eigenmode with the amplitude diverging linearly with the distance from the slab boundary. Remarkably, the slab reflectivity in such a situation can be very low, which means an almost 100% conversion of the incident light into the *axially frozen mode* with the electromagnetic energy density exceeding that of the incident wave by several orders of magnitude. The effect can be realized at any desirable frequency, including optical and UV frequency range. The only essential physical requirement is the presence of dielectric layers with proper oblique orientation of the anisotropy axes. Some practical aspects of this phenomenon are considered.

DOI: 10.1103/PhysRevE.68.036609 PACS number(s): 42.70.Qs, 41.20.−q, 84.40.−x

I. INTRODUCTION

Electromagnetic properties of periodic stratified media have been a subject of extensive research for decades (see, for example, Refs. [1–3], and references therein). Of particular interest has been the case of periodic stacks (one-dimensional photonic crystals) made up of lossless dielectric components with different refractive indices. Photonic crystals with one-dimensional periodicity had been widely used in optics long before the term ''photonic crystals'' was invented.

Let us look at the classical problem of a plane electromagnetic wave incident on the surface of semi-infinite plane-parallel periodic array, as shown in Fig. 1. The well-known effects of the slab periodicity are the following. (i) The possibility of omnidirectional reflectance when the incident radiation is reflected by the slab, regardless of the angle of incidence; (ii) the possibility of negative refraction, when the tangential component of the energy flux $\vec{S}_T$ of the transmitted wave is antiparallel to that of the incident wave; (iii) dramatic slowdown of the transmitted wave near photonic band edge frequency, where the normal component of the transmitted wave group velocity $\vec{u}$ vanishes along with the respective energy flux $\vec{S}_T$. An extensive discussion on the subject and numerous references can be found in Refs. [4–13]. All the above effects can occur even in the simplest case of a semi-infinite periodic array of two isotropic dielectric materials with different refractive indices, for example, glass and air. The majority of known photonic crystals fall into this category. The introduction of *dielectric anisotropy*, however, can bring qualitatively new features to electromagnetic properties of periodic stratified media and open up new opportunities for practical applications (see, for example, a recent publication [14]). One of such phenomena is the subject of this work.

A. The axially frozen mode

Consider a semi-infinite periodic stack with at least one of the constituents being an anisotropic dielectric material with oblique orientation of the anisotropic axis. A simple example of such an array is presented in Fig. 2. We will show that under certain physical conditions a monochromatic plane wave incident on the semi-infinite slab is converted into an abnormal electromagnetic mode with huge amplitude and nearly tangential energy density flux, as illustrated in Fig. 3. Such a wave will be referred to as the *axially frozen mode* (AFM). The use of this term is justified because the normal (axial) component u_z of the respective group velocity becomes vanishingly small, while the amplitude of the AFM can exceed the amplitude of the incident plane wave by several orders of magnitude.

The group velocity $\vec{u}$ of the AFM is parallel to the semi-infinite slab boundary and, therefore, the magnitude of the tangential component $(\vec{S}_T)_\perp$ of the respective energy density flux $\vec{S}_T$ is overwhelmingly larger than the magnitude of the normal component $(\vec{S}_T)_z$. But, although $(\vec{S}_T)_z \ll (\vec{S}_T)_\perp$, the normal component $(\vec{S}_T)_z$ of the energy density flux inside the

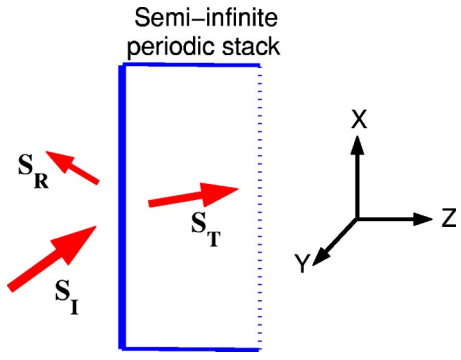

FIG. 1. The scattering problem for a semi-infinite periodic layered medium. $\vec{S}_I$, $\vec{S}_R$, and $\vec{S}_T$ are the energy density fluxes of the incident, reflected, and transmitted waves, respectively. The transmitted wave Ψ_T is a superposition of two Bloch eigenmodes, each of which can be either extended or evanescent. Only extended modes can transfer the energy in the z direction.

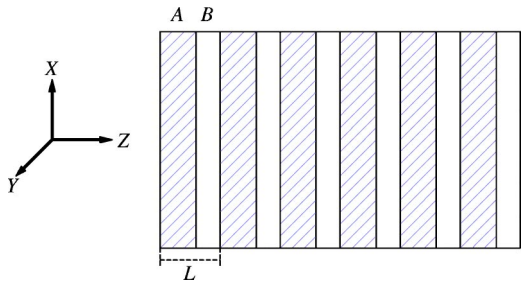

FIG. 2. Periodic layered structure with two layers A and B in a primitive cell L. The A layers (hatched) are anisotropic with one of the principle axes of the dielectric permittivity tensor $\hat{\varepsilon}$ making an oblique angle with the normal z to the layers ($\varepsilon_{xz}\neq 0$). The B layers are isotropic. The x-z plane coincides with the mirror plane m_y of the stack.

slab is still comparable with that of the incident plane wave in vacuum. This property persists even if the normal component u_z of the wave group velocity inside the slab vanishes, i.e.,

$$(\vec{S}_T)_z > 0 \quad \text{if} \quad u_z = 0. \tag{1}$$

The qualitative explanation for this is that the infinitesimally small value of u_z is offset by huge magnitude of the energy density W in the AFM. As the result, the product $u_z W$, which determines the normal component $(\vec{S}_T)_z$ of the energy flux, remains finite. The above behavior is totally different from what happens in the vicinity of a photonic band edge, where the normal component u_z of the wave group velocity vanishes too. Indeed, let us introduce the transmittance τ and the reflectance ρ of a lossless semi-infinite slab

$$\tau = 1-\rho = \frac{(\vec{S}_T)_z}{(\vec{S}_I)_z}, \quad \rho = -\frac{(\vec{S}_R)_z}{(\vec{S}_I)_z}. \tag{2}$$

In line with Eq. (1), in the AFM regime the transmittance τ remains significant and can be even close to unity, as shown in an example in Fig. 4(a). In other words, the incident plane wave enters the slab with little reflectance, where it turns into an abnormal AFM with an infinitesimally small normal component of the group velocity, huge amplitude, and a huge tangential component of the energy density flux. By contrast,

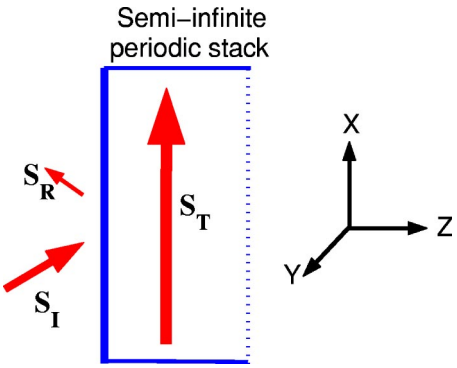

FIG. 3. An incident plane wave with unity energy density flux and a certain angle of incidence is converted into the AFM with huge amplitude, tangential group velocity, and nearly tangential energy flux $\vec{S}_T$. The normal components $(\vec{S}_I)_z$ and $(\vec{S}_T)_z$ of the incident and transmitted waves energy flux are comparable in magnitude.

in the vicinity of a photonic band edge [at frequencies near $\omega=\omega_b$ in Fig. 4(a)], the transmittance of the semi-infinite slab always vanishes, along with the normal component u_z of the wave group velocity.

It turns out that at a given frequency ω_0 the AFM regime can occur only for a special direction $\vec{n}_0$ of the incident plane wave propagation

$$\vec{n}_0 = \vec{n}_0(\omega_0). \tag{3}$$

This special direction of incidence always makes an oblique angle with the normal z to the layers. To find $\vec{n}_0$ for a given ω_0 or, conversely, to find ω_0 for a given $\vec{n}_0$, one has to solve the Maxwell equations in the periodic stratified medium. This problem will be addressed in Sec. III. In Sec. II we consider the relation between the AFM regime and the singularity of the electromagnetic dispersion relation responsible for such a peculiar behavior. If the frequency ω and the direction of incidence $\vec{n}$ do not match explicitly as prescribed by Eq. (3), the AFM regime will be somewhat smeared.

B. The vicinity of the AFM regime

Let $\Psi_T(z)$ be the transmitted electromagnetic field inside the semi-infinite slab (the explicit definition of $\Psi_T(z)$ is

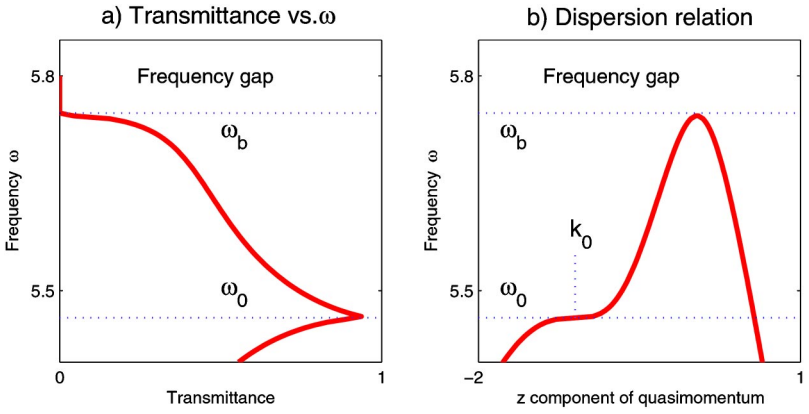

FIG. 4. (a) The transmittance τ of periodic semi-infinite slab vs frequency at fixed direction $\vec{n}$ of the incidence. At the frequency ω_0 of the AFM, τ is close to unity, which implies that the incident wave almost completely gets converted into the AFM. (b) The respective axial dispersion relation $\omega(k_z)$ at fixed (n_x,n_y) from Eq. (12). At $k_z=k_0$ and $\omega=\omega_0$ this spectral branch develops a stationary inflection point (16) associated with the AFM regime. ω_b is the edge of the frequency band for a given (n_x,n_y). The values of ω and k are expressed in units of c/L and $1/L$, respectively.

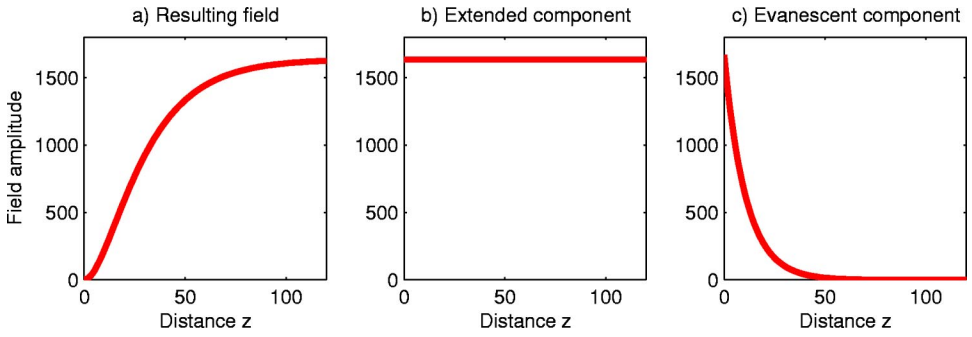

FIG. 5. Destructive interference of the extended and evanescent components of the resulting electromagnetic field (4) inside semi-infinite slab in close proximity of the AFM regime: (a) the amplitude $|\Psi_T(z)|^2$ of the resulting field, (b) the amplitude $|\Psi_{ex}(z)|^2$ of the extended contribution, (c) the amplitude $|\Psi_{ev}(z)|^2$ of the evanescent contribution. The amplitude $|\Psi_I|^2$ of the incident wave is unity. The distance z from the slab boundary is expressed in units of L.

given in Eqs. (38) and (88)]. It turns out that in the vicinity of the AFM regime, $\Psi_T(z)$ is a superposition of the extended and evanescent Bloch eigenmodes

$$\Psi_T(z)=\Psi_{ex}(z)+\Psi_{ev}(z), \quad z>0, \tag{4}$$

where $\Psi_{ex}(z)$ is an extended mode with $u_z>0$, and $\Psi_{ev}(z)$ is an evanescent mode with Im $k_z>0$. As shown in an example in Fig. 5, both the contributions to $\Psi_T(z)$ have huge and nearly equal and opposite values near the slab boundary, so that their superposition (4) at $z=0$ is small enough to satisfy the boundary condition (90). As the distance z from the slab boundary increases, the evanescent component $\Psi_{ev}(z)$ decays exponentially, while the amplitude of the extended component $\Psi_{ex}(z)$ remains constant and huge. As the result, the field amplitude $|\Psi_T(z)|^2$ reaches its huge saturation value $|\Psi_{ex}|^2$ at a certain distance from the slab boundary [see Eqs. (99), (100), and (101)].

When the direction of incidence $\vec{n}$ tends to its critical value $\vec{n}_0$ for a given frequency ω_0, the respective saturation value $|\Psi_{ex}|^2$ of the AFM amplitude $|\Psi_T(z)|^2$ diverges as $|\vec{n}-\vec{n}_0|^{-2/3}$. Conversely, when the frequency ω tends to its critical value ω_0 for a given direction of incidence $\vec{n}_0$, the saturation value of the AFM amplitude diverges as $|\omega-\omega_0|^{-2/3}$. In the real situation, of course, the AFM amplitude will be limited by such physical factors as (i) nonlinear effects, (ii) electromagnetic losses, (iii) structural imperfections of the periodic array, (iv) finiteness of the slab dimensions, (v) deviation of the incident radiation from a perfect plane monochromatic wave.

Figure 6 gives a good qualitative picture of what really happens in the vicinity of the AFM regime. Consider a wide monochromatic beam of frequency ω incident on the surface of semiinfinite photonic slab. The direction of incidence $\vec{n}_0 \| \vec{S}_I$ is chosen so that condition (3) of the AFM regime is satisfied at $\omega=\omega_0$. As frequency ω tends to ω_0 from either direction, the normal component u_z of the transmitted wave group velocity approaches zero, while the tangential component $\vec{u}_\perp$ remains finite

$$u_z \sim |\omega-\omega_0|^{2/3} \to 0, \quad \vec{u}_\perp \to \vec{u}_0 \quad \text{as} \quad \omega \to \omega_0. \tag{5}$$

This relation together with the equality

$$\frac{\pi}{2}-\theta_T=\arctan\frac{u_z}{u_\perp}, \tag{6}$$

involving the refraction angle θ_T, yield

$$\frac{\pi}{2}-\theta_T \sim |\omega-\omega_0|^{2/3} \to 0 \quad \text{as} \quad \omega \to \omega_0. \tag{7}$$

Hence, in the vicinity of the AFM regime, the transmitted (refracted) electromagnetic wave can be viewed as a *grazing mode*. The most important and unique feature of this grazing mode directly relates to the fact that the transmittance τ of the semi-infinite slab remains finite even at $\omega=\omega_0$ [see, for example, Fig. 4(a)]. Indeed, let A_I and A_T be the cross-

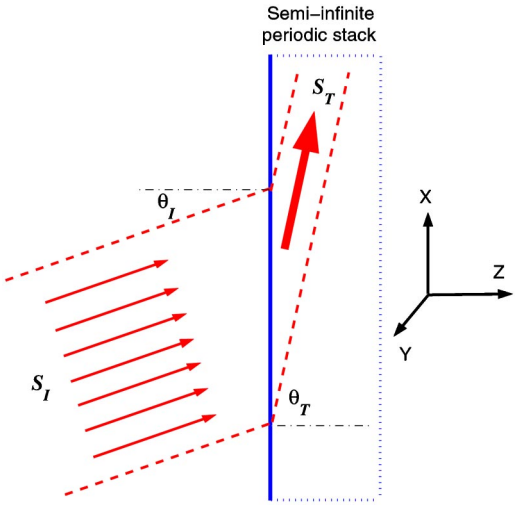

FIG. 6. Incident and transmitted (refracted) waves in the vicinity of the AFM regime. The reflected wave is not shown. θ_I and θ_T are the incidence and refraction angles, S_I and S_T are the energy density fluxes of the incident and transmitted waves. Both the energy density and the energy density flux in the transmitted wave are much larger than the respective values in the incident wave. However, the total power transmitted by the refracted wave is smaller by factor τ, due to much smaller cross-section area of the nearly grazing transmitted wave.

section areas of the incident and transmitted (refracted) beams, respectively. Obliviously,

$$\frac{A_T}{A_I}=\frac{\cos\theta_T}{\cos\theta_I}. \tag{8}$$

Let us also introduce the quantities

$$U_I=A_IS_I, \quad U_T=A_TS_T, \tag{9}$$

where S_I and S_T are the energy density fluxes of the incident and transmitted waves. U_I and U_T are the total power transmitted by the incident and transmitted (refracted) beams, respectively. Expressions (8) and (9) imply that

$$\frac{U_T}{U_I}=\frac{S_T\cos\theta_T}{S_I\cos\theta_I}=\frac{(S_T)_z}{(S_I)_z}=\tau, \tag{10}$$

which is nothing more than a manifestation of the energy conservation law. Finally, Eq. (10), together with formula (7), yield

$$S_T=\tau S_I\frac{\cos\theta_I}{\cos\theta_T}\sim|\omega-\omega_0|^{-2/3}\to\infty \quad \text{as} \quad \omega\to\omega_0, \tag{11}$$

where we have taken into account that $\tau S_I\cos\theta_I$ is limited (of the order of magnitude of unity) as $\omega\to\omega_0$. By contrast, in the vicinity of the photonic band edge the transmittance τ of the semi-infinite slab vanishes along with the energy density flux S_T of the transmitted (refracted) wave.

Expressions (7) and (11) show that in the vicinity of the AFM regime the transmitted wave behaves like a grazing mode with huge and nearly tangential energy density flux S_T and very small (compared to that of the incident beam) cross-section area A_T, so that the total power $U_T=A_TS_T$ associated with the transmitted wave cannot exceed the total power U_I of the incident wave: $U_T=\tau U_I\leqslant U_I$.

The above qualitative consideration is only valid on the scales exceeding the size L of the unit cell (which is of the order of magnitude of c/ω) and more importantly, exceeding the *transitional distance* $l=(\mathrm{Im}\,k_{ev})^{-1}$ from the slab boundary where the evanescent mode contribution to the resulting electromagnetic field $\Psi_T(z)$ is still significant. The latter means that the width of both the incident and the refracted beam must be much larger than l. If the above condition is not met, we cannot treat the transmitted wave as a beam, and expressions (7)–(11) do not apply. Instead, we would have to use the explicit electrodynamic expressions for $\Psi_T(z)$, such as the asymptotic formula (101). Note that if the direction $\vec{n}$ of the incident wave propagation and the frequency ω *exactly match* condition (3) for the AFM regime, the transmitted wave $\Psi_T(z)$ does not reduce to superposition (4) of canonical Bloch eigenmodes. Instead, the AFM is described by a general Floquet eigenmode $\Psi_{01}(z)$ from Eq. (80), which diverges inside the slab as z, until the nonlinear effects or other limiting factors come into play. The related mathematical analysis is provided in Secs. III and IV.

In some respects, the remarkable behavior of the AFM is similar to that of the frozen mode related to the phenomenon of *electromagnetic unidirectionality* in nonreciprocal magnetic photonic crystals [15,16]. In a unidirectional photonic crystal, electromagnetic radiation of a certain frequency ω_0 can propagate with finite group velocity $\vec{u}\|z$ only in one of the two opposite directions, say, from right to left. The problem with the electromagnetic unidirectionality, though, is that it essentially requires the presence of magnetic materials with strong circular birefringence (Faraday rotation) and low losses at the frequency range of interest. Such materials are readily available at the microwave frequencies, but at the infrared and optical frequency ranges, finding appropriate magnetic materials is highly problematic. Thus, at frequencies above 10^{12} Hz, the electromagnetic unidirectionality along with the respective nonreciprocal magnetic mechanism of the frozen mode formation may prove to be impractical. By contrast, the occurrence of AFM *does not* require the presence of magnetic or any other essentially dispersive components in the periodic stack. Therefore, the AFM regime *can be realized* at any frequencies, including the infrared, optical, and even ultraviolet frequency ranges. The only essential physical requirement is the presence of anisotropic dielectric layers with proper orientation of the anisotropy axes. An example of such an array is shown in Fig. 2.

In Sec. II we establish the relation between the phenomenon of AFM and the electromagnetic dispersion relation of the periodic layered medium. This allows us to formulate strict and simple symmetry conditions for such a phenomenon to occur, as well as to find out what kind of periodic stratified media can exhibit the effect. Relevant theoretical analysis based on the Maxwell equations in stratified media is carried out in Secs. III and IV. Finally, in Sec. V we discuss some practical aspects of the phenomenon.

II. DISPERSION RELATION WITH THE AFM

Now we establish the connection between the phenomenon of AFM and the electromagnetic dispersion relation $\omega(\vec{k})$, $\vec{k}=(k_x,k_y,k_z)$ of the periodic stratified medium. In a plane-parallel stratified slab, the tangential components (k_x,k_y) of the Bloch wave vector $\vec{k}$ always coincide with those of the incident plane wave in Figs. 1, 3, and 6 while the normal component k_z is different from that of the incident wave. To avoid confusion, in further consideration the z component of the Bloch wave vector $\vec{k}$ inside the periodic slab will be denoted as k without the subscript z, namely,

$$\text{inside periodic stack:} \quad \vec{k}=(k_x,k_y,k).$$

The value of k is found by solving the Maxwell equations in the periodic stratified medium for given ω and (k_x,k_y); k is defined up to a multiple of $2\pi/L$, where L is the period of the layered structure.

Consider now the frequency ω as function of k for fixed (k_x,k_y). A typical example of such a dependence is shown in Fig. 7(a). A large gap at the lowest frequencies is determined by the value of the fixed tangential components (k_x,k_y) of the quasimomentum $\vec{k}$. This gap vanishes in the case of normal incidence, when $k_x=k_y=0$. An alternative and more

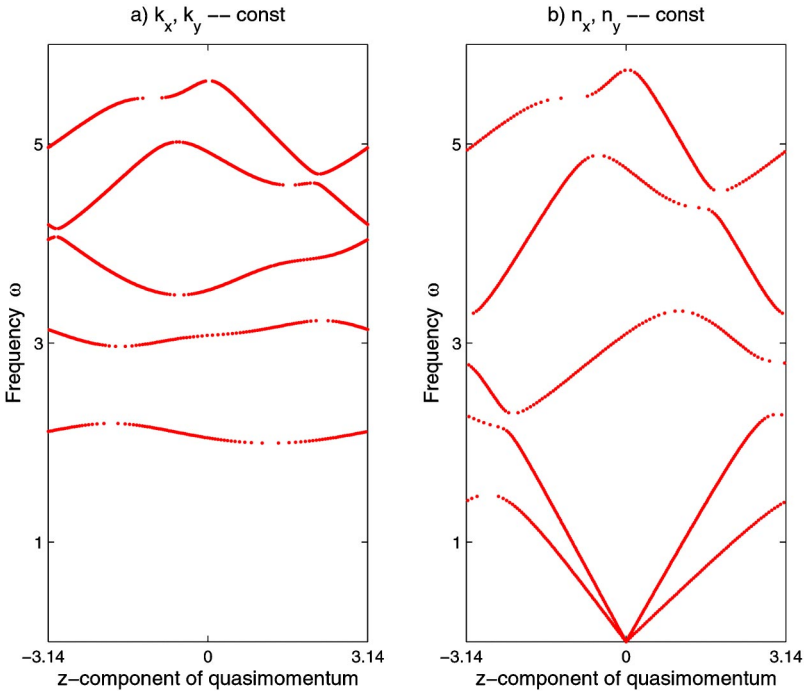

FIG. 7. The axial dispersion relation of anisotropic periodic stack in Fig. 2: (a) $\omega(k_z)$ for fixed values (k_x,k_y) of the tangential components of quasimomentum $\vec{k}$; (b) $\omega(k_z)$ for fixed values (n_x,n_y), defining the direction of incidence. In the case of normal incidence, there would be no difference between (a) and (b).

convenient representation for the dispersion relation is presented in Fig. 7(b), where the plot of $\omega(k)$ is obtained for fixed (n_x,n_y) based on

$$(n_x,n_y)=(ck_x/\omega,ck_y/\omega). \tag{12}$$

The pair of values (n_x,n_y) coincide with the tangential components of the unit vector $\vec{n}$ defining the direction of the incident plane wave propagation. The dependence $\omega(k)$ for fixed (n_x,n_y) or for fixed (k_x,k_y) will be referred to as the *axial dispersion relation*.

Suppose that for $\vec{k}=\vec{k}_0$ and $\omega=\omega_0=\omega(\vec{k}_0)$, one of the spectral branches $\omega(k)$ develops a stationary inflection point for given $(k_x,k_y)=(k_{0x},k_{0y})$, i.e.,

$$\left(\frac{\partial\omega}{\partial k}\right)_{k_x,k_y}\Bigg|_{\vec{k}=\vec{k}_0}=0;\quad \left(\frac{\partial^2\omega}{\partial k^2}\right)_{k_x,k_y}\Bigg|_{\vec{k}=\vec{k}_0}=0;$$
$$\left(\frac{\partial^3\omega}{\partial k^3}\right)_{k_x,k_y}\Bigg|_{\vec{k}=\vec{k}_0}\neq 0. \tag{13}$$

The value

$$u_z=\left(\frac{\partial\omega}{\partial k}\right)_{k_x,k_y} \tag{14}$$

in Eq. (13) is the axial component of the group velocity, which vanishes at $\vec{k}=\vec{k}_0$. Observe that

$$u_x=\left(\frac{\partial\omega}{\partial k_x}\right)_{k,k_y}\quad\text{and}\quad u_y=\left(\frac{\partial\omega}{\partial k_y}\right)_{k,k_x}, \tag{15}$$

representing the tangential components of the group velocity, may not be zeros at $\vec{k}=\vec{k}_0$.

Notice that instead of Eq. (13) one can use another definition of the stationary inflection point

$$\left(\frac{\partial\omega}{\partial k}\right)_{n_x,n_y}\Bigg|_{\vec{k}=\vec{k}_0}=0,\quad \left(\frac{\partial^2\omega}{\partial k^2}\right)_{n_x,n_y}\Bigg|_{\vec{k}=\vec{k}_0}=0,$$
$$\left(\frac{\partial^3\omega}{\partial k^3}\right)_{n_x,n_y}\Bigg|_{\vec{k}=\vec{k}_0}\neq 0. \tag{16}$$

The partial derivatives in Eqs. (16) are taken at constant (n_x,n_y), rather than at constant (k_x,k_y). Observe that definitions (13) and (16) are equivalent, and we will use both of them.

In Fig. 4(b) we reproduced an enlarged fragment of the upper spectral branch of the axial dispersion relation in Fig. 7(b). For the chosen (n_x,n_y), this branch develops a stationary inflection point (16) at $\omega=\omega_0$ and $k=k_0$. The extended Bloch eigenmode with $\omega=\omega_0$ and $\vec{k}=\vec{k}_0$, associated with the stationary inflection point, turns out to be directly related to the AFM.

In Secs. III and IV, based on the Maxwell equations, we prove that singularity (16) [or, equivalently, Eq. (13)] indeed leads to the very distinct AFM regime in the semi-infinite periodic stack. We also show that a necessary condition for such a singularity and, therefore, a necessary condition for the AFM existence is the following property of the axial dispersion relation of the periodic stack:

$$\omega(k_x,k_y,k)\neq\omega(k_x,k_y,-k)$$

or, equivalently,

$$\omega(n_x,n_y,k)\neq\omega(n_x,n_y,-k). \tag{17}$$

This property will be referred to as the *axial spectral asymmetry*. Evidently, the axial dispersion relations presented in Fig. 7 satisfy this criterion. Leaving the proof of the above statements to Sec. III, let us look at the constraints imposed by criterion (17) on the geometry and composition of the periodic stack.

A. Conditions for the axial spectral asymmetry

First of all notice that a periodic array would definitely have an *axially symmetric* dispersion relation

$$\omega(k_x,k_y,k)=\omega(k_x,k_y,-k)$$

or, equivalently,

$$\omega(n_x,n_y,k)=\omega(n_x,n_y,-k), \tag{18}$$

if the symmetry group G of the periodic stratified medium includes any of the following two symmetry operations:

$$m_z,2_z'=2_z\times R, \tag{19}$$

where m_z is the mirror plane parallel to the layers, 2_z is the twofold rotation about the z axis, and R is the time reversal operation. Indeed, since $2_z(k_x,k_y,k)=(-k_x,-k_y,k)$ and $R(k_x,k_y,k)=(-k_x,-k_y,-k)$, we have

$$2_z'(k_x,k_y,k)=(k_x,k_y,-k),$$

which implies relation (18) for arbitrary (k_x,k_y). The same is true for the mirror plane m_z,

$$m_z(k_x,k_y,k)=(k_x,k_y,-k).$$

Consequently, a necessary condition for the axial spectral asymmetry (17) of a periodic stack is the absence of the symmetry operations (19), i.e.,

$$m_z\notin G \quad \text{and} \quad 2_z'\notin G. \tag{20}$$

In reciprocal (nonmagnetic) media, where by definition $R\in G$, instead of Eq. (20), one can use the following requirement:

$$m_z\notin G \quad \text{and} \quad 2_z\notin G. \tag{21}$$

Note, that the *axial spectral symmetry* (18) is different from the *bulk spectral symmetry*

$$\omega(k_x,k_y,k)=\omega(-k_x,-k_y,-k). \tag{22}$$

For example, the space inversion I and/or the time reversal R, if present in G, ensure the bulk spectral symmetry (22), but neither I nor R ensures the axial spectral symmetry (18).

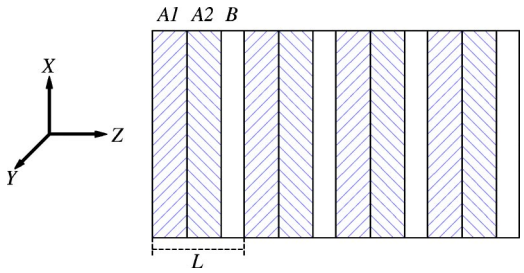

FIG. 8. Periodic stack composed of anisotropic layers $A1$ and $A2$, which are the mirror images of each other, and isotropic layers B. This stack has axially symmetric dispersion relation and does not support the AFM regime. This is true even if the B layers are removed.

Application of criterion (21) to different periodic stacks

Condition (21) for the axial spectral asymmetry imposes certain restrictions on the geometry and composition of the periodic stratified medium, as well as on the direction of the incident wave propagation.

a. Restrictions on the geometry and composition of the periodic stack. First of all, observe that a common periodic stack made up of *isotropic* dielectric components with different refractive indices always has axially symmetric dispersion relation (18), no matter how complicated the periodic array is or how many different isotropic materials are involved. To prove this, it suffices to note that such a stack always supports the symmetry operation 2_z.

In fact, the symmetry operation 2_z holds in the more general case when all the layers are either isotropic or have a purely *in-plane* anisotropy

$$\hat{\boldsymbol{\varepsilon}}=\begin{bmatrix}\varepsilon_{xx} & \varepsilon_{xy} & 0\\ \varepsilon_{xy} & \varepsilon_{yy} & 0\\ 0 & 0 & \varepsilon_{zz}\end{bmatrix}. \tag{23}$$

Obviously, the in-plane anisotropy (23) does not remove the symmetry operation 2_z and, therefore, property (18) of the axial spectral symmetry holds in this case. Thus, we can state that in order to display the axial spectral asymmetry, the periodic stack must include at least one anisotropic component, either uniaxial or biaxial. In addition, one of the principle axes of the respective dielectric permittivity tensor $\hat{\varepsilon}$ must make an oblique angle with the normal to the layers, which means that *at least one of the two components ε_{xz} and ε_{yz} of the respective dielectric tensor must be nonzero*.

The above requirement gives us a simple and useful idea on what kind of periodic stratified media can support the axial spectral asymmetry and the AFM regime. But this is not a substitute for the stronger symmetry criterion (20) or (21). For example, although the periodic stack in Fig. 8 includes the A layers identical to those in Fig. 2, this stack does not meet criterion (20) for the axial spectral asymmetry. Indeed, the stack in Fig. 8 supports the mirror plane m_z, which, according to expression (19), ensures the axial spectral symmetry.

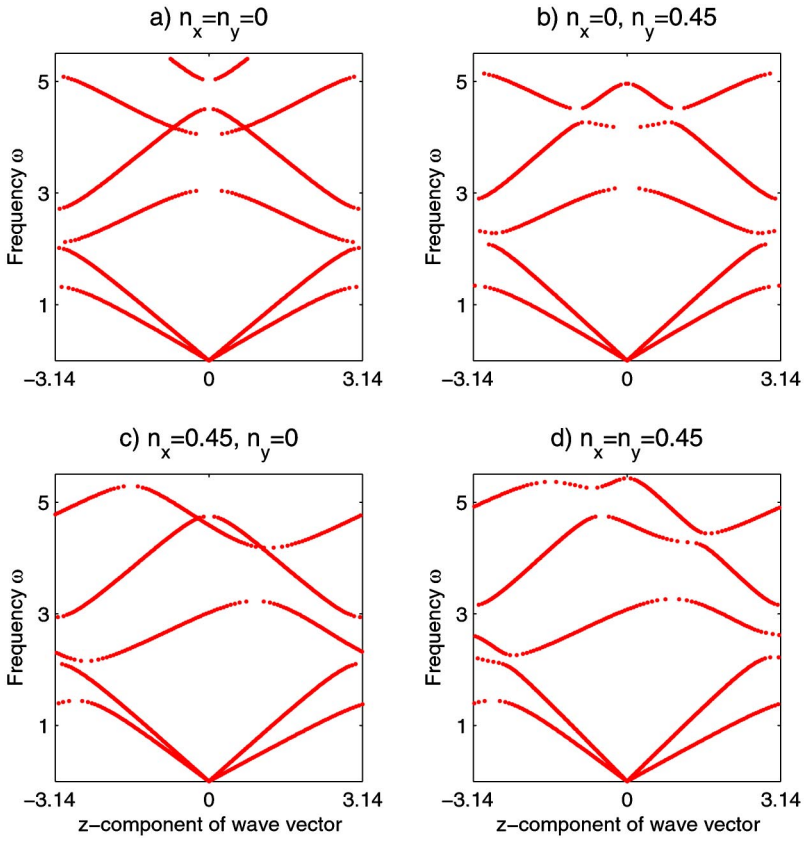

FIG. 9. Axial dispersion relation $\omega(k)$ for fixed (n_x, n_y) for the periodic array in Fig. 2. The AFM regime can occur only if $n_x \neq 0$ and $n_y \neq 0$ [the case (d)].

b. Restriction on the direction of incident wave propagation. Consider now an important particular case $k_x = k_y = 0$ of the normal incidence. Criterion (17) reduces now to the simple requirement

$$\omega(\vec{k}) \neq \omega(-\vec{k}), \tag{24}$$

[where $\vec{k} = (0,0,k)$] of the bulk spectral asymmetry, which is prohibited in nonmagnetic photonic crystals due to the time reversal symmetry. Therefore, in the nonmagnetic case, we have the following additional condition for the axial spectral asymmetry:

$$k_\perp = \sqrt{k_x^2 + k_y^2} \neq 0, \tag{25}$$

implying that the AFM cannot be excited in a nonmagnetic semi-infinite stack by a normally incident plane wave, i.e., *the incident angle must be oblique*.

Conditions (21) and (25) may not be necessary in the case of nonreciprocal magnetic stacks (see the details in Ref. [15]). But as we mentioned earlier, at frequencies above 10^{12} Hz, the nonreciprocal effects in common nonconducting materials are negligible. Therefore, in order to have a robust AFM regime in the infrared or optical frequency range, we must satisfy both requirements (21) and (25), regardless of whether or not nonreciprocal magnetic materials are involved.

As soon as the above conditions are met, one can always achieve the AFM regime at any desirable frequency ω within a certain frequency range $\Delta\omega$. The frequency range $\Delta\omega$ is determined by the stack geometry and the dielectric materials used, while a specific value of ω within the range can be selected by the direction $\vec{n}$ of the light incidence.

B. Periodic stack with two layers in unit cell

The simplest and the most practical example of a periodic stack supporting the axial spectral asymmetry (17) and, thereby, the AFM regime is shown in Fig. 2. It is made up of anisotropic A layers alternated with isotropic B layers. The respective dielectric permittivity tensors are

$$\hat{\varepsilon}_A = \begin{bmatrix} \varepsilon_{xx} & 0 & \varepsilon_{xz} \\ 0 & \varepsilon_{yy} & 0 \\ \varepsilon_{xz} & 0 & \varepsilon_{zz} \end{bmatrix}, \quad \hat{\varepsilon}_B = \begin{bmatrix} \varepsilon_B & 0 & 0 \\ 0 & \varepsilon_B & 0 \\ 0 & 0 & \varepsilon_B \end{bmatrix}. \tag{26}$$

For simplicity, we assume

$$\hat{\mu}_A = \hat{\mu}_B = \hat{I}. \tag{27}$$

The stack in Fig. 2 has the monoclinic symmetry

$$2_y / m_y \tag{28}$$

with the mirror plane m_y normal to the y axis. Such a symmetry is compatible with the necessary condition (21) for the AFM existence. But as we will see below, symmetry (28) imposes additional constraints on the direction $\vec{n}$ of the incident wave propagation.

In Fig. 9 we show the axial dispersion relation $\omega(k)$ of this periodic array, computed for four different directions

(n_x, n_y) of incident wave propagation. These four cases cover all the possibilities, different in terms of symmetry.

In case (a) of normal incidence, when $n_x = n_y = 0$, the dispersion relation is axially symmetric, as must be the case with any reciprocal periodic stratified medium [see the explanation after Eq. (24)].

In the case (b), when $n_x = 0$ and $n_y \neq 0$, the two necessary conditions (21) and (25) for the axial spectral asymmetry are met. Yet, those conditions prove not to be sufficient. Indeed, if $n_x = 0$, either of the symmetry operations

$$2_y \quad \text{and} \quad m_y' \equiv m_y \times R \tag{29}$$

imposes the relation

$$\omega(0, k_y, k) = \omega(0, k_y, -k), \tag{30}$$

which implies the axial spectral symmetry. Neither stationary inflection point, nor AFM can occur in this case.

In case (c), when $n_x \neq 0$ and $n_y = 0$, the situation is more complicated. The quasimomentum $\vec{k}$ lies now in the x-z plane, which coincides with the mirror plane m_y. Therefore, every Bloch eigenmode $\Psi_{\vec{k}}(z)$ can be classified as a pure TE or pure TM mode, depending on the $\Psi_{\vec{k}}(z)$ parity with respect to the mirror reflection m_y:

$$\text{for TE mode} \quad m_y \Psi_{\vec{k}}(z) = -\Psi_{\vec{k}}(z);$$

$$\text{for TM mode} \quad m_y \Psi_{\vec{k}}(z) = \Psi_{\vec{k}}(z). \tag{31}$$

The TE modes have axially symmetric dispersion relation

$$\omega(k_x, 0, k) = \omega(k_x, 0, -k). \tag{32}$$

Indeed, the component ε_{xz} of the dielectric tensor $\hat{\varepsilon}_A$ does not affect the TE modes, because in this case the electric component $\mathbf{E}(\mathbf{r}, t)$ of the electromagnetic field is parallel to the y axis. As a consequence, the axial dispersion relation of the TE spectral branches is similar to that of the isotropic case with $\varepsilon_{xz} = 0$, where it is always symmetric. By contrast, for the TM modes we have $\mathbf{E}(\mathbf{r}, t) \perp y$. Therefore, the TM modes are affected by ε_{xz} and display axially asymmetric dispersion relation

$$\omega(k_x, 0, k) \neq \omega(k_x, 0, -k), \tag{33}$$

as seen in Fig. 9(c). We wish to remark, though, that equality (32) cannot be derived from symmetry arguments only. The axial spectral symmetry of the TE modes is not exact and relies on approximation (27) for the magnetic permeability of the A layers. On the other hand, the fact that the spectral branches have different parity (31) with respect to the symmetry operation m_y implies that none of the branches can develop a stationary inflection point [see Eq. (83) and explanations thereafter]. Thus, in the case $n_y = 0$, in spite of the axial spectral asymmetry, the AFM regime cannot occur either.

Finally, in the general case (d), when $n_x \neq 0$ and $n_y \neq 0$, all the spectral branches display property (17) of the axial spectral asymmetry. In addition, the Bloch eigenmodes now are of the same symmetry [23]—neither TE, nor TM. This is exactly the case when the AFM regime can be achieved at some frequencies by proper choice of the incident angle. For instance, if we impose the equality $n_x = n_y$ and change the incident angle only, it turns out that every single spectral branch at some point develops a stationary inflection point (16) and, thereby, displays the AFM at the respective frequency. If we want the AFM at a specified frequency ω_0, then we will have to adjust both n_x and n_y.

III. ELECTRODYNAMICS OF THE AXIALLY FROZEN MODE

A. Reduced Maxwell equations

We start with the classical Maxwell equations for time-harmonic fields in nonconducting media

$$\nabla \times \mathbf{E}(\vec{r}) = i \frac{\omega}{c} \mathbf{B}(\vec{r}), \quad \nabla \times \mathbf{H}(\vec{r}) = -i \frac{\omega}{c} \mathbf{D}(\vec{r}), \tag{34}$$

where

$$\mathbf{D}(\vec{r}) = \hat{\varepsilon}(\vec{r}) \mathbf{E}(\vec{r}), \quad \mathbf{B}(\vec{r}) = \hat{\mu}(\vec{r}) \mathbf{H}(\vec{r}). \tag{35}$$

In a lossless dielectric medium, the material tensors $\hat{\varepsilon}(\vec{r})$ and $\hat{\mu}(\vec{r})$ are Hermitian. In a stratified medium, the tensors $\hat{\varepsilon}(\vec{r})$ and $\hat{\mu}(\vec{r})$ depend on a single Cartesian coordinate z, and the Maxwell equations (34) can be recast as

$$\nabla \times \mathbf{E}(\vec{r}) = i \frac{\omega}{c} \hat{\mu}(z) \mathbf{H}(\vec{r}), \quad \nabla \times \mathbf{H}(\vec{r}) = -i \frac{\omega}{c} \hat{\varepsilon}(z) \mathbf{E}(\vec{r}). \tag{36}$$

Solutions for Eq. (36) are sought in the following form:

$$\mathbf{E}(\vec{r}) = e^{i(k_x x + k_y y)} \vec{E}(z), \quad \mathbf{H}(\vec{r}) = e^{i(k_x x + k_y y)} \vec{H}(z). \tag{37}$$

Substitution (37) transforms the system of six linear equation (36) into a system of four linear differential equations

$$\partial_z \Psi(z) = i \frac{\omega}{c} M(z) \Psi(z), \quad \Psi(z) = \begin{bmatrix} E_x(z) \\ E_y(z) \\ H_x(z) \\ H_y(z) \end{bmatrix}. \tag{38}$$

The explicit expression for the Maxwell operator $M(z)$ is

$$M(z) = \begin{bmatrix} M_{11} & M_{12} \\ M_{21} & M_{22} \end{bmatrix}, \tag{39}$$

where

$$M_{11} = \begin{bmatrix} -\dfrac{\varepsilon_{xz}^*}{\varepsilon_{zz}} n_x - \dfrac{\mu_{yz}}{\mu_{zz}} n_y & \left(-\dfrac{\varepsilon_{yz}^*}{\varepsilon_{zz}} + \dfrac{\mu_{yz}}{\mu_{zz}} \right) n_x \\ -\left(\dfrac{\varepsilon_{xz}^*}{\varepsilon_{zz}} - \dfrac{\mu_{xz}}{\mu_{zz}} \right) n_y & -\dfrac{\varepsilon_{yz}^*}{\varepsilon_{zz}} n_y - \dfrac{\mu_{xz}}{\mu_{zz}} n_x \end{bmatrix},$$

$$M_{22}=\begin{bmatrix} -\frac{\varepsilon_{yz}}{\varepsilon_{zz}}n_y-\frac{\mu^*_{xz}}{\mu_{zz}}n_x & \left(\frac{\varepsilon_{yz}}{\varepsilon_{zz}}-\frac{\mu^*_{yz}}{\mu_{zz}}\right)n_x \\ \left(\frac{\varepsilon_{xz}}{\varepsilon_{zz}}-\frac{\mu^*_{xz}}{\mu_{zz}}\right)n_y & -\frac{\varepsilon_{xz}}{\varepsilon_{zz}}n_x-\frac{\mu^*_{yz}}{\mu_{zz}}n_y \end{bmatrix},$$

$$M_{12}=\begin{bmatrix} \mu^*_{xy}-\frac{\mu^*_{xz}\mu_{yz}}{\mu_{zz}}+\frac{n_xn_y}{\varepsilon_{zz}} & \mu_{yy}-\frac{\mu_{yz}\mu^*_{yz}}{\mu_{zz}}-\frac{n_x^2}{\varepsilon_{zz}} \\ -\mu_{xx}+\frac{\mu_{xz}\mu^*_{xz}}{\mu_{zz}}+\frac{n_y^2}{\varepsilon_{zz}} & -\mu_{xy}+\frac{\mu_{xz}\mu^*_{yz}}{\mu_{zz}}-\frac{n_xn_y}{\varepsilon_{zz}} \end{bmatrix},$$

$$M_{21}=\begin{bmatrix} -\varepsilon^*_{xy}+\frac{\varepsilon^*_{xz}\varepsilon_{yz}}{\varepsilon_{zz}}-\frac{n_xn_y}{\mu_{zz}} & -\varepsilon_{yy}+\frac{\varepsilon_{yz}\varepsilon^*_{yz}}{\varepsilon_{zz}}+\frac{n_x^2}{\mu_{zz}} \\ \varepsilon_{xx}-\frac{\varepsilon_{xz}\varepsilon^*_{xz}}{\varepsilon_{zz}}-\frac{n_y^2}{\mu_{zz}} & \varepsilon_{xy}-\frac{\varepsilon_{xz}\varepsilon^*_{yz}}{\varepsilon_{zz}}+\frac{n_xn_y}{\mu_{zz}} \end{bmatrix}.$$

The Cartesian components of the material tensors $\hat{\varepsilon}$ and $\hat{\mu}$ are functions of z and (in dispersive media) ω. The reduced Maxwell equation (38) should be complemented with the following expressions for the z components of the fields:

$$E_z=(-n_xH_y+n_yH_x-\varepsilon^*_{13}E_x-\varepsilon^*_{23}E_y)\varepsilon_{zz}^{-1},$$

$$H_z=(n_xE_y-n_yE_x-\mu^*_{13}H_x-\mu^*_{23}H_y)\mu_{zz}^{-1}, \qquad (40)$$

where (n_x,n_y) are defined in Eq. (12).

Notice that in the case of normal incidence, the Maxwell operator is drastically simplified

$$M_{11}=M_{22}=0 \quad \text{for} \quad n_x=n_y=0. \qquad (41)$$

This is the case we dealt with in Ref. [16] when considering the phenomenon of electromagnetic unidirectionality in nonreciprocal magnetic photonic crystals. By contrast, the objective of this section is to show how the terms M_{11} and M_{22}, occurring only in the case of oblique incidence [24], can lead to the phenomenon of AFM, regardless of whether or not the nonreciprocal effects are present.

Importantly, the 4×4 matrix $M(z)$ in Eq. (39) has the property of J Hermitivity defined as

$$(JM)^\dagger=JM, \qquad (42)$$

where

$$J=J^{-1}=\begin{bmatrix} 0 & 0 & 0 & 1 \\ 0 & 0 & -1 & 0 \\ 0 & -1 & 0 & 0 \\ 1 & 0 & 0 & 0 \end{bmatrix}. \qquad (43)$$

Different versions of the reduced Maxwell equation (38) can be found in the extensive literature on electrodynamics of stratified media (see, for example, Refs. [17–19], and references therein). For more detailed studies of J-Hermitian and J-unitary operators see Ref. [20].

B. The transfer matrix

The Cauchy problem

$$\partial_z\Psi(z)=i\frac{\omega}{c}M(z)\Psi(z), \quad \Psi(z_0)=\Psi_0 \qquad (44)$$

for the reduced Maxwell equation (38) has a unique solution

$$\Psi(z)=T(z,z_0)\Psi(z_0), \qquad (45)$$

where the 4×4 matrix $T(z,z_0)$ is so-called *transfer matrix*. From definition (45) of the transfer matrix it follows that

$$T(z,z_0)=T(z,z')T(z',z_0), \quad T(z,z_0)=T^{-1}(z_0,z),$$
$$T(z,z)=I. \qquad (46)$$

The matrix $T(z,z_0)$ is uniquely defined by the following Cauchy problem:

$$\partial_zT(z,z_0)=i\frac{\omega}{c}M(z)T(z,z_0), \quad T(z,z)=I. \qquad (47)$$

Equation (47), together with J-Hermitivity (42) of the Maxwell operator $M(z)$, implies that the matrix $T(z,z_0)$ is J *unitarity*, i.e.,

$$T^\dagger(z,z_0)=JT^{-1}(z,z_0)J \qquad (48)$$

(see the proof in Appendix A). The J-unitarity (48) of the transfer matrix imposes strong constraints on its eigenvalues [see Eq. (61)]. It also implies that

$$|\det T(z,z_0)|=1. \qquad (49)$$

The transfer matrix T_S of a stack of layers is a sequential product of the transfer matrices T_m of the constitutive layers

$$T_S=\prod_m T_m. \qquad (50)$$

If the individual layers are homogeneous, the corresponding single-layer transfer matrices T_m are explicitly expressed in terms of the respective Maxwell operators M_m:

$$T_m=\exp(iz_mM_m), \qquad (51)$$

where z_m is the thickness of the mth layer. The explicit expression for M_m is given by Eq. (39). Thus, formula (50), together with Eqs. (51) and (39), gives us an explicit expression for the transfer matrix T_S of an arbitrary stack of anisotropic dielectric layers. T_S is a function of (i) the material tensors $\hat{\varepsilon}$ and $\hat{\mu}$ in each layer of the stack, (ii) the layer thicknesses, (iii) the frequency ω, and (iv) the tangential components $(k_x,k_y)=(n_x\omega/c,n_y\omega/c)$ of the wave vector.

Consider the important particular case of normal wave propagation. Using Eq. (51) and the explicit expression (39) for the Maxwell operator, one can prove that

$$\det(T_S)=1 \quad \text{for} \quad n_x=n_y=0. \qquad (52)$$

Additional information related to the transfer matrix formalism can be found in Refs. [17–19] and references therein.

C. Periodic arrays: Bloch eigenmodes

In a periodic layered structure, all material tensors, along with the J-Hermitian matrix $M(z)$ in Eq. (38), are periodic functions of z;

$$M(z+L)=M(z), \tag{53}$$

where L is the length of a primitive cell of the periodic stack. By definition, Bloch solutions $\Psi_k(z)$ of the reduced Maxwell equation (38) with the periodic operator $M(z)$ satisfy

$$\Psi_k(z+L)=e^{ikL}\Psi_k(z). \tag{54}$$

Definition (45) of the T matrix together with Eq. (54) give

$$\Psi_k(z+L)=T(z+L,z)\Psi_k(z)=e^{ikL}\Psi_k(z). \tag{55}$$

Introducing the transfer matrix of a primitive cell

$$T_L=T(L,0), \tag{56}$$

we have from Eq. (55)

$$T_L\Phi_k=e^{ikL}\Phi_k, \tag{57}$$

where $\Phi_k=\Psi_k(0)$. Thus, the eigenvectors of the transfer matrix T_L of the unit cell are uniquely related to the eigenmodes of the reduced Maxwell equation (38) through the relations

$$\Phi_{k_1}=\Psi_{k_1}(0), \quad \Phi_{k_2}=\Psi_{k_2}(0),$$

$$\Phi_{k_3}=\Psi_{k_3}(0), \quad \Phi_{k_4}=\Psi_{k_4}(0). \tag{58}$$

The respective four eigenvalues

$$X_i=e^{ik_iL}, \quad i=1,2,3,4 \tag{59}$$

of T_L are the roots of the characteristic equation

$$F(X)=0, \tag{60}$$

where $F(X)=\det(T_L-X\hat{I})=X^4+P_3X^3+P_2X^2+P_1X+1$. For any given ω and (k_x,k_y), the characteristic equation defines a set of four values $\{X_1,X_2,X_3,X_4\}$, or equivalently, $\{k_1,k_2,k_3,k_4\}$. Real k correspond to propagating Bloch waves (extended modes), while complex k correspond to evanescent modes. Evanescent modes are relevant near photonic crystal boundaries and other structural irregularities.

The J-unitarity (48) of T_L imposes the following restriction on eigenvalues (59) for any given ω and (k_x,k_y):

$$\{k_i\}\equiv\{k_i^*\}, \quad i=1,2,3,4. \tag{61}$$

In view of relation (61), one has to consider three different situations. The first possibility

$$k_1\equiv k_1^*, \quad k_2\equiv k_2^*, \quad k_3\equiv k_3^*, \quad k_4\equiv k_4^* \tag{62}$$

relates to the case of all four Bloch eigenmodes being extended. The second possibility

$$k_1=k_1^*, \quad k_2=k_2^*, \quad k_3=k_4^*, \tag{63}$$

where $k_3\neq k_3^*$, $k_4\neq k_4^*$, relates to the case of two extended and two evanescent modes. The last possibility

$$k_1=k_2^*, \quad k_3=k_4^*, \tag{64}$$

where $k_1\neq k_1^*$, $k_2\neq k_2^*$, $k_3\neq k_3^*$, $k_4\neq k_4^*$, relates the case of a frequency gap, when all four Bloch eigenmodes are evanescent.

Observe that the relation

$$k_1+k_2+k_3+k_4\equiv 0,$$

valid in the case of normal incidence (see Refs. [15,16]), may not apply now.

Axial spectral symmetry

Assume that the transfer matrix T_L is similar to its inverse

$$T_L=U^{-1}T_L^{-1}U, \tag{65}$$

where U is an invertible 4×4 matrix. This assumption together with property (48) of J unitarity imply the similarity of T_L and $T_L^\dagger$

$$T_L=V^{-1}T_L^\dagger V, \tag{66}$$

where $V=JU$. This relation imposes additional restrictions on eigenvalues (59) for a given frequency ω and given (k_x,k_y)

$$\{k_i\}\equiv\{-k_i\}, \quad i=1,2,3,4. \tag{67}$$

Relation (67) is referred to as the axial spectral symmetry, because in terms of the corresponding axial dispersion relation, it implies equality (18) for every spectral branch.

If the sufficient condition (65) for the axial spectral symmetry is not in place, then we can have for a given ω and (k_x,k_y)

$$\{k_i\}\neq\{-k_i\}, \quad i=1,2,3,4 \tag{68}$$

which implies the axial spectral asymmetry (17).

D. Stationary inflection point

The coefficients of the characteristic polynomial $F(X)$ in Eq. (60) are functions of ω and (k_x,k_y). Let $F_0(X)$ be the characteristic polynomial at the stationary inflection point (16), where $\omega=\omega_0$ and $(k_x,k_y)=(k_{0x},k_{0y})$. The stationary inflection point (16) can also be defined as follows

$$F_0(X)=0, \quad F_0'(X)=0, \quad F_0''(X)=0, \quad F_0'''(X)\neq 0. \tag{69}$$

This relation requires the respective value of $X_0=\exp(ik_0L)$ to be a triple root of the characteristic polynomial $F_0(X)$ implying

$$F_0(X)=(X-X_1)(X-X_0)^3=0. \tag{70}$$

A small deviation of the frequency ω from its critical value ω_0 changes the coefficients of the characteristic polynomial and removes the triple degeneracy of the solution X_0,

$$X-X_0\approx -6^{1/3}\left(\frac{\partial F_0/\partial\omega}{\partial^3 F_0/\partial X^3}\right)^{1/3}(\omega-\omega_0)^{1/3}\xi,$$

$$\xi=1,e^{2\pi i/3},e^{-2\pi i/3} \tag{71}$$

or, in terms of the axial quasimomentum k,

$$k-k_0\approx 6^{1/3}\left(\frac{\omega-\omega_0}{\omega_0'''}\right)^{1/3}\xi,\quad \xi=1,e^{2\pi i/3},e^{-2\pi i/3}, \tag{72}$$

where

$$\omega_0'''=\left(\frac{\partial^3\omega}{\partial k^3}\right)_{k_x,k_y}\Bigg|_{\vec{k}=\vec{k}_0}>0. \tag{73}$$

The three solutions (72) can also be rearranged as

$$k_{ex}\approx k_0+6^{1/3}(\omega_0''')^{-1/3}(\omega-\omega_0)^{1/3},$$

$$k_{ev}\approx k_0+\frac{1}{2}(6)^{1/3}(\omega_0''')^{-1/3}(\omega-\omega_0)^{1/3}$$

$$+i\frac{\sqrt{3}}{2}6^{1/3}(\omega_0''')^{-1/3}|\omega-\omega_0|^{1/3},$$

$$k_{EV}\approx k_0+\frac{1}{2}(6)^{1/3}(\omega_0''')^{-1/3}(\omega-\omega_0)^{1/3}$$

$$-i\frac{\sqrt{3}}{2}6^{1/3}(\omega_0''')^{-1/3}|\omega-\omega_0|^{1/3}. \tag{74}$$

The real k_{ex} in Eq. (74) relates to the extended mode $\Psi_{ex}(z)$, with $u_z=0$ at $\omega=\omega_0$. The other two solutions, k_{ev} and $k_{EV}=k_{ev}^*$, correspond to a pair of evanescent modes $\Psi_{ev}(z)$ and $\Psi_{EV}(z)$ with positive and negative infinitesimally small imaginary parts, respectively. Those modes are truly evanescent (i.e., have Im $k\neq 0$) only if $\omega\neq\omega_0$, but it does not mean that at $\omega=\omega_0$ the eigenmodes $\Psi_{ev}(z)$ and $\Psi_{EV}(z)$ become extended. In what follows we will take a closer look at this problem.

Eigenmodes at the frequency of AFM

Consider the vicinity of stationary inflection point (13). As long as $\omega\neq\omega_0$, the four eigenvectors (58) of the transfer matrix T_L comprise two extended and two evanescent Bloch solutions. One of the extended modes (say, Φ_{k_1}) corresponds to the nondegenerate real root $X_1=e^{ik_1L}$ of the characteristic equation (60). This mode has negative axial group velocity $u_z(k_1)<0$ and, therefore, is of no interest for us. The other three eigenvectors of T_L correspond to three nearly degenerate roots (71). As ω approaches ω_0, these three eigenvalues become degenerate, while the respective three eigenvectors Φ_{k_2}, Φ_{k_3}, and Φ_{k_4} become collinear,

$$\Phi_{k_2}\to\alpha_1\Phi_{k_0},\quad \Phi_{k_3}\to\alpha_2\Phi_{k_0},\quad \Phi_{k_4}\to\alpha_3\Phi_{k_0},$$

$$\text{as}\quad \omega\to\omega_0. \tag{75}$$

The latter important feature relates to the fact that at $\omega=\omega_0$ the matrix T_L has a nontrivial Jordan canonical form

$$U^{-1}T_LU=\begin{bmatrix} X_1 & 0 & 0 & 0\\ 0 & X_0 & 1 & 0\\ 0 & 0 & X_0 & 1\\ 0 & 0 & 0 & X_0\end{bmatrix}, \tag{76}$$

and, therefore, cannot be diagonalized. It is shown rigorously in Ref. [16] that the very fact that the T_L eigenvalues display singularity (71) implies that at $\omega=\omega_0$ the matrix T_L has the canonical form (76). In line with Eq. (75), the matrix T_L from Eq. (76) has only two (not four) eigenvectors: (1) $\Phi_{k_1}=\Psi_{k_1}(0)$, corresponding to the nondegenerate root X_1 and relating to the extended mode with $u_z<0$; (2) $\Phi_{k_0}=\Psi_{k_0}(0)$, corresponding to the triple root X_0 and related to the AFM.

The other two solutions of the Maxwell equation (38) at $\omega=\omega_0$ are general Floquet eigenmodes, which do not reduce to the canonical Bloch form (54). Yet, they can be related to $\Psi_{k_0}(z)$. Indeed, following the standard procedure (see, for example, Refs. [21,22]), consider an extended Bloch solution $\Psi_k(z)$ of the reduced Maxwell equation (38)

$$\mathbf{L}\Psi_k(z)=0, \tag{77}$$

where $\mathbf{L}=\partial_z-i(\omega/c)M(z)$, where both operators $M(z)$ and $\mathbf{L}(z)$ are functions of ω and (k_x,k_y). Assume now that the axial dispersion relation $\omega(k)$ has a stationary inflection point (13) at $k=k_0$. Differentiating Eq. (77) with respect to k at constant (k_x,k_y) gives, with consideration for Eq. (13),

$$\mathbf{L}\partial_k\Psi_k(z)=0,\quad \mathbf{L}\partial_{kk}^2\Psi_k(z)=0,\quad \text{at}\quad k=k_0.$$

This implies that at $k=k_0$, both functions

$$\Psi_{01}(z)=\partial_k\Psi_k(z)\big|_{k=k_0}\ \text{ and }\ \Psi_{02}(z)=\partial_{kk}^2\Psi_k(z)\big|_{k=k_0} \tag{78}$$

are also eigenmodes of the reduced Maxwell equation at $\omega=\omega_0$. Representing $\Psi_k(z)$ in the form

$$\Psi_k(z)=\psi_k(z)e^{ikz}, \tag{79}$$

where $\psi_k(z+L)=\psi_k(L)$, Im $k=0$, and substituting Eq. (79) into Eq. (78) we get

$$\Psi_{01}(z)=\overline{\Psi}_{k_0}(z)+iz\Psi_{k_0}(z), \tag{80}$$

$$\Psi_{02}(z)=\overline{\Psi}'_{k_0}(z)+iz\overline{\Psi}_{k_0}(z)-z^2\Psi_{k_0}(z), \tag{81}$$

where

$$\overline{\Psi}_{k_0}(z)=[\partial_k\psi_k(z)]_{k=k_0}e^{ik_0z}$$

and

$$\overline{\Psi}'_{k_0}(z)=[\partial^2_{kk}\psi_k(z)]_{k=k_0}e^{ik_0z}$$

are auxiliary Bloch functions (not eigenmodes).

To summarize, at the frequency ω_0 of AFM, there are four solutions for the reduced Maxwell equation (38),

$$\Psi_{k_1}(z),\quad \Psi_{k_0}(z),\quad \Psi_{01}(z),\quad \Psi_{02}(z). \tag{82}$$

The first two solutions from Eq. (82) are extended Bloch eigenmodes with $u_z<0$ and $u_z=0$, respectively. The other two solutions diverge as the first and the second power of z, respectively, they are referred to as general (non-Bloch) Floquet modes.

Deviation of the frequency ω from ω_0 removes the triple degeneracy (76) of the matrix T_L, as seen from Eq. (71). The modified matrix T_L can now be reduced to a diagonal form with the set (58) of four eigenvectors comprising two extended and two evanescent Bloch solutions.

E. Symmetry considerations

In Sec. II, we discussed the relation between the symmetry of the axial dispersion relation of a periodic stack, and the phenomenon of AFM. At this point we can prove that indeed the axial spectral asymmetry (17) is a necessary condition for the occurrence of the stationary inflection point and for the AFM associated with such a point. As we have seen earlier in this section, the stationary inflection point relates to a triple root of the characteristic polynomial $F(X)$ from Eq. (60). Since $F(X)$ is a polynomial of the fourth degree, it cannot have a symmetric pair of triple roots, that would have been the case for axially symmetric dispersion relation. Hence, only asymmetric axial dispersion relation $\omega(k)$ can display a stationary inflection point (13) or, equivalently, Eq. (16), as shown in Fig. 4(b). In this respect, the situation with the AFM is somewhat similar to that of the frozen mode in unidirectional magnetic photonic crystals [16]. The difference lies in the physical nature of the phenomenon. The bulk spectral asymmetry (24) leading to the effect of electromagnetic unidirectionality, essentially requires the presence of nonreciprocal magnetic materials. By contrast, the axial spectral asymmetry (17) along with the AFM regime can be realized in perfectly reciprocal periodic dielectric stacks with symmetric bulk dispersion relation (22). On the other hand, the axial spectral asymmetry essentially requires an oblique light incidence, which is not needed for the bulk spectral asymmetry.

Another important symmetry consideration is that in the vicinity of the stationary inflection point (13), all four Bloch eigenmodes (58) must have the same symmetry, which means that all of them must belong to the same one-dimensional irreducible representation of the Bloch wave vector group. This condition is certainly met when the direction defined by (n_x,n_y) is not special in terms of symmetry. Let us see what happens if the above condition is not in place. Consider situation (31), when at any given frequency ω and fixed $(n_x,n_y)=(n_x,0)$, two of the Bloch eigenmodes are TE modes and the other two are TM modes. Note, that TE and TM modes belong to *different* one-dimensional representations of the Bloch wave vector group. In such a case, the transfer matrix T_L can be reduced to the block-diagonal form

$$T_L=\begin{bmatrix} T_{11} & T_{12} & 0 & 0\\ T_{21} & T_{22} & 0 & 0\\ 0 & 0 & T_{33} & T_{34}\\ 0 & 0 & T_{43} & T_{44}\end{bmatrix}.$$

The respective characteristic polynomial $F(X)$ degenerates into

$$F(X)=F_{TE}(X)F_{TM}(X), \tag{83}$$

where $F_{TE}(X)$ and $F_{TM}(X)$ are independent second degree polynomials describing the TE and TM spectral branches, respectively. Obviously, in such a situation, the transfer matrix cannot have the nontrivial canonical form (76), and the respective axial dispersion relation cannot develop a stationary inflection point (69), regardless of whether or not the axial spectral asymmetry is in place.

IV. THE AFM REGIME IN A SEMI-INFINITE STACK

A. Boundary conditions

In vacuum (to the left of semi-infinite slab in Fig. 1) the electromagnetic field $\Psi_V(z)$ is a superposition of the incident and reflected waves

$$\Psi_V(z)=\Psi_I(z)+\Psi_R(z),\quad \text{at } z<0. \tag{84}$$

At the slab boundary we have

$$\Psi_V(0)=\Psi_I(0)+\Psi_R(0)=\Phi_I+\Phi_R, \tag{85}$$

where

$$\Phi_I=\begin{bmatrix} E_{I,x}\\ E_{I,y}\\ H_{I,x}\\ H_{I,y}\end{bmatrix}=\begin{bmatrix} E_{I,x}\\ E_{I,y}\\ -E_{I,x}n_xn_yn_z^{-1}-E_{I,y}(1-n_x^2)n_z^{-1}\\ E_{I,x}(1-n_y^2)n_z^{-1}+E_{I,y}n_xn_yn_z^{-1}\end{bmatrix},$$

$$\Phi_R=\begin{bmatrix} E_{R,x}\\ E_{R,y}\\ H_{R,x}\\ H_{R,y}\end{bmatrix}=\begin{bmatrix} E_{R,x}\\ E_{R,y}\\ E_{R,x}n_xn_yn_z^{-1}+E_{R,y}(1-n_x^2)n_z^{-1}\\ -E_{R,x}(1-n_y^2)n_z^{-1}-E_{R,y}n_xn_yn_z^{-1}\end{bmatrix}. \tag{86}$$

The complex vectors $\vec{E}_I,\vec{H}_I$ and $\vec{E}_R,\vec{H}_R$ are related to the actual electromagnetic field components $\mathbf{E}_I,\mathbf{H}_I$ and $\mathbf{E}_R,\mathbf{H}_R$ as

$$\mathbf{E}_I=e^{i\omega/c(n_xx+n_yy)}\vec{E}_I(z),\quad \mathbf{H}_I=e^{i\omega/c(n_xx+n_yy)}\vec{H}_I,$$

$$\mathbf{E}_R = e^{i\omega/c(n_x x + n_y y)}\vec{E}_R(z), \quad \mathbf{H}_R = e^{i\omega/c(n_x x + n_y y)}\vec{H}_R .$$

The transmitted wave $\Psi_T(z)$ inside the semi-infinite slab is a superposition of two Bloch eigenmodes [25],

$$\Psi_T(z) = \Psi_1(z) + \Psi_2(z), \quad \text{at } z>0. \tag{87}$$

The eigenmodes $\Psi_1(z)$ and $\Psi_2(z)$ can be both extended (with $u_x>0$), one extended and one evanescent (with $u_x>0$ and Im $k>0$, respectively), or both evanescent (with Im $k>0$), depending on which of the three cases (62), (63), or (64) we are dealing with. In particular, in the vicinity of the AFM [e.g., the vicinity of ω_0 in Fig. 4(b)], we always have situation (63). Therefore, in the vicinity of AFM, $\Psi_T(z)$ is a superposition of the extended eigenmode $\Psi_{ex}(z)$ with the group velocity $u_z>0$, and the evanescent mode $\Psi_{ev}(z)$ with Im $k>0$

$$\Psi_T(z) = \Psi_{ex}(z) + \Psi_{ev}(z), \quad \text{at } z>0. \tag{88}$$

The asymptotic expressions for the respective wave vectors k_{ex} and k_{ev} in the vicinity of AFM are given in Eq. (74).

When the frequency ω exactly coincides with the frequency ω_0 of the AFM, representation (88) for $\Psi_T(z)$ is not valid. In such a case, according to Eq. (74), there are no evanescent modes at all. It turns out that at $\omega=\omega_0$, the electromagnetic field inside the slab is a superposition of the extended mode $\Psi_{k_0}(z)$ and the (non-Bloch) Floquet eigenmode $\Psi_{01}(z)$ from Eq. (80)

$$\Psi_T(z) = \Psi_{k_0}(z) + \Psi_{01}(z), \quad \text{at } \omega=\omega_0 \quad \text{and} \quad z>0. \tag{89}$$

Since the extended eigenmode $\Psi_{k_0}(z)$ has zero axial group velocity u_z, it does not contribute to the axial energy flux S_z. By contrast, the divergent non-Bloch contribution $\Psi_{01}(z)$ is associated with the finite axial energy flux $S_z>0$, although the notion of group velocity does not apply here. A detailed analysis is carried out below.

Knowing the eigenmodes inside the slab and using the standard electromagnetic boundary conditions

$$\Phi_T = \Phi_I + \Phi_R , \tag{90}$$

where $\Phi=\Psi(0)$, one can express the amplitude and composition of the transmitted wave Ψ_T and reflected wave Ψ_R, in terms of the amplitude and polarization of the incident wave Ψ_I. This gives us the transmittance and reflectance coefficients (2) of the semi-infinite slab, as well as the electromagnetic field distribution $\Psi_T(z)$ inside the slab, as functions of the incident wave polarization, the direction $\vec{n}$ of incidence, and the frequency ω.

B. Field amplitude inside the semi-infinite slab

In what follows we assume that ω can be arbitrarily close but not equal to ω_0, unless otherwise is explicitly stated. This will allow us to treat the transmitted wave $\Psi_T(z)$ as a superposition (88) of one extended and one evanescent mode. Since evanescent modes do not transfer energy in the z direction, the extended mode is solely responsible for the axial energy flux S_z

$$S_z(\Psi_T) = S_z(\Psi_{ex}). \tag{91}$$

According to Eq. (B3), S_z does not depend on z and can be expressed in terms of the semi-infinite slab transmittance τ from Eq. (2)

$$S_z = \tau(\vec{S}_I)_z = \tau S_I , \tag{92}$$

where $S_I=(\vec{S}_I)_z$ is the axial energy flux of the incident wave, which is set to be unity.

The energy density W_{ex} associated with the extended mode $\Psi_{ex}(z)$ can be expressed in terms of the axial component u_z of its group velocity and the axial component $S_z(\Psi_{ex})$ of the respective energy density flux

$$W_{ex} = u_z^{-1} S_z(\Psi_{ex}) = \left(\frac{\partial\omega}{\partial k}\right)^{-1}_{k_x,k_y} \tau S_I . \tag{93}$$

In close proximity of the AFM frequency ω_0, we have, according to Eq. (13),

$$\omega - \omega_0 \approx \frac{1}{6}\omega_0'''(k-k_0)^3, \tag{94}$$

where ω_0''' is defined in Eq. (73). Differentiating Eq. (94) with respect to k

$$\left(\frac{\partial\omega}{\partial k}\right)_{k_x,k_y} \approx \frac{1}{2}\omega_0'''(k-k_0)^2 \approx \frac{6^{2/3}}{2}(\omega_0''')^{1/3}(\omega-\omega_0)^{2/3}, \tag{95}$$

and plugging Eq. (95) into Eq. (93) yields

$$W_{ex} \approx \frac{2}{6^{2/3}}\tau S_I(\omega_0''')^{-1/3}(\omega-\omega_0)^{-2/3}, \tag{96}$$

where the transmittance τ depends on the incident wave polarization, the frequency ω, and the direction of incidence $(n_x,n_y)=(ck_x/\omega, ck_y/\omega)$. Formula (96) implies that the energy density W_{ex} and, therefore, the amplitude $|\Psi_{ex}(z)| = |\Phi_{ex}|$ of the extended mode inside the stack diverge in the vicinity of the AFM regime

$$|\Phi_{ex}| \sim \sqrt{W_{ex}} \sim \sqrt{\tau S_I}(\omega_0''')^{-1/6}|\omega-\omega_0|^{-1/3} \quad \text{as} \quad \omega\to\omega_0 . \tag{97}$$

The divergence of the extended mode amplitude $|\Phi_{ex}|$ imposes the similar behavior on the amplitude $|\Psi_{ev}(0)| = |\Phi_{ev}|$ of the evanescent mode at the slab boundary. Indeed, the boundary condition (90) requires that the resulting field $\Phi_T=\Phi_{ex}+\Phi_{ev}$ remains limited to match the sum $\Phi_I+\Phi_R$ of the incident and reflected waves. Relation (90) together with Eq. (97) imply that there is a destructive interference of the extended Φ_{ex} and evanescent Φ_{ev} modes at the stack boundary,

$$\Phi_{ex} \approx -\Phi_{ev} \approx K\sqrt{\tau S_I}(\omega_0''')^{-1/6}(\omega-\omega_0)^{-1/3}\Phi_{k_0} \quad \text{as} \quad \omega\to\omega_0, \tag{98}$$

Here Φ_{k_0} is the normalized eigenvector of T_L in Eq. (76); K is a dimensionless parameter. Expression (98) is in compliance with the earlier made statement (75) that the column vectors Φ_{ex} and Φ_{ev} become collinear as $\omega\to\omega_0$.

1. Space distribution of electromagnetic field in the AFM regime

The amplitude $|\Psi_{ex}(z)|$ of the extended Bloch eigenmode remains constant and equal to $|\Phi_{ex}|$ from Eq. (97), while the amplitude of the evanescent contribution to the resulting field decays as

$$|\Psi_{ev}(z)| = |\Phi_{ev}| e^{-z\ \mathrm{Im}\, k_{ev}}, \tag{99}$$

where $\mathrm{Im}\, k_{ev} \approx \sqrt{3}/2 6^{1/3}(\omega_0''')^{-1/3}|\omega-\omega_0|^{1/3}$. At $z \gg (\mathrm{Im}\, k_{ev})^{-1}$, the destructive interference (98) of the extended and evanescent modes becomes ineffective, and the only remaining contribution to $\Psi_T(z)$ is the extended mode $\Psi_{ex}(z)$ with huge and independent of z amplitude (97). This situation is graphically demonstrated in Fig. 5.

Let us see what happens when the frequency ω tends to its critical value ω_0. According to Eqs. (57) and (88), at $z=NL$, $N=0,1,2,\ldots$, the resulting field $\Psi_T(z)$ inside the slab can be represented as

$$\Psi_T(z) = \Phi_{ex} e^{izk_{ex}} + \Phi_{ev} e^{izk_{ev}}. \tag{100}$$

Substituting k_{ex} and k_{ev} from Eq. (74) in Eq. (100), and taking into account the asymptotic relation (98), we have

$$\Psi_T(z) \approx \left[\Phi_T + zK\sqrt{\frac{\tau S_I}{\omega_0'''}}6^{1/3} \times\left(\frac{i}{2}+\frac{\sqrt{3}}{2}\frac{\omega-\omega_0}{|\omega-\omega_0|}\right)\Phi_{k_0}\right] e^{izk_0} \quad \text{as} \quad \omega\to\omega_0. \tag{101}$$

Although this asymptotic formula is valid only for $z=NL$, $N=0,1,2,\ldots$, it is obviously consistent with expression (80) for the non-Bloch solution $\Psi_{10}(z)$ of the Maxwell equation (38) at $\omega=\omega_0$.

2. The role of the incident wave polarization

The incident wave polarization affects the relative contributions of the extended and evanescent components to the resulting field $\Psi_T(z)$ in Eq. (88). In addition, it also affects the overall transmittance (2). The situation here is similar to that of the normal incidence considered in Ref. [16]. There are two special cases, merging into a single one as $\omega\to\omega_0$. The first one occurs when the elliptic polarization of the incident wave is chosen so that it produces a single extended eigenmode $\Psi_{ex}(z)$ inside the slab [no evanescent contribution to $\Psi_T(z)$]. In this case, $\Psi_T(z)$ reduces to $\Psi_{ex}(z)$, and its amplitude $|\Psi_T(z)|$ remains limited and independent of z. As ω approaches ω_0, the respective transmittance τ vanishes in this case, and there is no AFM regime. The second special case is when the elliptic polarization of the incident wave is chosen so that it produces a single evanescent eigenmode $\Psi_{ev}(z)$ inside the slab [no extended contribution to $\Psi_T(z)$]. In such a case, $\Psi_T(z)$ reduces to $\Psi_{ev}(z)$, and the amplitude $|\Psi_T(z)|$ decays exponentially with z in accordance with Eq. (99). The respective transmittance τ in this latter case is zero regardless of the frequency ω, because evanescent modes do not transfer energy. Importantly, as ω approaches ω_0, the polarizations of the incident wave that produce either a sole extended or a sole evanescent mode become indistinguishable, in accordance with Eq. (75). In the vicinity of the AFM regime, the maximal transmittance τ is achieved for the incident wave polarization orthogonal to that exciting a single extended or evanescent eigenmode inside the semi-infinite stack.

C. Tangential energy flux

So far we have been focusing on the axial electromagnetic field distribution, as well as the axial energy flux S_z inside the semi-infinite slab. At the same time, in and near the AFM regime, the overwhelmingly stronger energy flux occurs in the tangential direction. Let us take a closer look at this problem.

The axial energy flux S_z is exclusively provided by the extended contribution $\Psi_{ex}(z)$ to the resulting field $\Psi_T(z)$, because the evanescent mode $\Psi_{ev}(z)$ does not contribute to S_z. Neither $|\Psi_{ex}|$ nor S_z depends on z [see Eq. (B3)]. By contrast, both the extended and the evanescent modes determine the tangential energy flux $\vec{S}_\tau(z)$. Besides, according to Eq. (B3), the tangential energy flux depends on z. Far from the AFM regime, the role of the evanescent mode is insignificant, because $\Psi_{ev}(z)$ is appreciable only in a narrow region close to the slab boundary. But the situation appears quite different near the AFM frequency. Indeed, according to Eq. (99), the imaginary part of the respective Bloch wave vector k_{ev} becomes infinitesimally small near the critical point. As a consequence, the evanescent mode extends deep inside the slab, so does its role in formation of $\vec{S}_\tau(z)$. The tangential energy flux $\vec{S}_\tau(z)$ as function of z can be directly obtained using formula (B5) and the explicit expression for $\Psi_T(z)=\Psi_{ex}(z)+\Psi_{ev}(z)$. Although the explicit expression for $\vec{S}_\tau(z)$ is rather complicated and cumbersome, it has very simple and transparent structure. Indeed, the tangential energy flux can be represented in the following form:

$$\vec{S}_\tau(z) = \vec{u}_\tau W(z),$$

where the tangential group velocity $\vec{u}_\tau$ behaves regularly at $\omega=\omega_0$. Therefore, the magnitude and the space distribution of the tangential energy flux $\vec{S}_\tau(z)$ in and near the AFM regime literally coincide with that of the electromagnetic energy density $W(z)$, which is proportional to $|\Psi_T(z)|^2$. A typical picture of that is shown in Fig. 5(a).

V. SUMMARY

As we have seen in the preceding section, a distinctive characteristic of the AFM regime is that the incident monochromatic radiation turns into a very unusual grazing wave inside the slab, as shown schematically in Figs. 3 and 6. Such a grazing wave is significantly different from that occurring in the vicinity of the total internal reflection regime, where the transmitted wave also propagates along the interface. The most obvious difference is that near the regime of total internal reflection, the reflectivity approaches unity, which implies that the intensity of the transmitted (refracted) wave vanishes. By contrast, in the case of AFM the light reflection from the interface can be small, as shown in an example in Fig. 4(a). Thus, in the AFM case, a significant portion of the incident light gets converted into the grazing wave (the AFM) with huge amplitude, compared to that of the incident wave. For this reason, the AFM regime can be of great utility in many applications.

Another distinctive feature of the AFM regime relates to the field distribution inside the periodic medium. The electromagnetic field of the AFM can be approximated by a divergent Floquet eigenmode $\Psi_{10}(z)$ from Eq. (80), whose magnitude $|\Psi_{10}(z)|^2$ increases as z^2, until nonlinear effects or other limiting factors come into play. In fact, the field amplitude inside the slab can exceed the amplitude of the incident plane wave by several orders of magnitude, depending on the quality of the periodic array, the actual number of the layers, and the width of the incident light beam.

Looking at the z component of light group velocity and energy flux, we see a dramatic slowdown of light in the vicinity of the AFM regime, with all possible practical applications extensively discussed in the literature (see, for example, Refs. [9–12], and references therein). In principle, there can be a situation when the tangential components (u_x, u_y) of the group velocity also vanish in the AFM regime, along with the axial component u_z. Although we did not try to achieve such a situation in our numerical experiments, it is not prohibited and might occur if the physical parameters of the periodic array are chosen properly. In such a case, the AFM regime reduces to its particular case—the frozen mode regime with $\vec{u}=0$ inside the periodic medium. This regime would be similar to that considered in Ref. [16], with one important difference: it is not related to the magnetic unidirectionality and, hence, there is no need to incorporate nonreciprocal magnetic layers in the periodic array. The latter circumstances allow to realize the frozen mode regime at the infrared, optical, and even UV frequency range.

ACKNOWLEDGMENTS

The efforts of A. Figotin and I. Vitebskiy were sponsored by the Air Force Office of Scientific Research, Air Force Materials Command, USAF, under Grant No. F49620-01-1-0567.

APPENDIX A: *J* UNITARITY OF THE TRANSFER MATRIX

Let $n\times n$ matrix $T(z)$ satisfy the following Cauchy problem:

$$\partial_z T(z) = iM(z)T(z), \quad T(0)=I \tag{A1}$$

where $M(z)$ is a J-Hermitian matrix. Let us prove that the unique solution $T(z)$ for Eq. (A1) is a J-unitary operator,

$$T^{\dagger}(z) = JT^{-1}(z)J^{-1}. \tag{A2}$$

To prove it, notice that Eq. (A1) implies

$$\partial_x T^{\dagger}(z) = -T^{\dagger}(x)iA(z)J, \quad T^{\dagger}(0)=I, \tag{A3}$$

where $A(z)=JM(z)$ is a Hermitian matrix. Now, let us find the respective Cauchy problem for $T^{-1}(z)$. Since

$$\partial_z[T(z)T^{-1}(z)] = 0 = T(z)[\partial_z T^{-1}(z)] + [\partial_z T(z)]T^{-1}(z),$$

we have

$$\partial_z T^{-1}(z) = -T^{-1}(z)[\partial_z T(z)]T^{-1}(z),$$

which in a combination with Eq. (A1) yields

$$\partial_z T^{-1}(z) = -T^{-1}(z)iJA(z), \quad T^{-1}(0)=I. \tag{A4}$$

Finally, multiplying both sides of equality (A4) by J and using the fact that $J^2=I$, we get the following Cauchy problem for $JT^{-1}(z)J$:

$$\partial_z[JT^{-1}(z)J] = -[JT^{-1}(z)J]iA(z)J, \quad JT^{-1}(0)J=I \tag{A5}$$

which is identical to that for $T^{\dagger}(z)$ from Eq. (A3). Since both Cauchy problems (A3) and (A5) have unique solutions, their similarity implies relation (A2) of J unitarity.

APPENDIX B: ENERGY DENSITY FLUX

The real-valued Poynting vector is defined by

$$\mathbf{S}(\vec{r}) = \frac{c}{8\pi}\mathrm{Re}[\mathbf{E}^*(\vec{r})\times\mathbf{H}(\vec{r})]. \tag{B1}$$

Substituting representation (37) for $\mathbf{E}(\vec{r})$ and $\mathbf{H}(\vec{r})$ in Eq. (B1) yields

$$\mathbf{S}(\vec{r}) = \mathbf{S}(z) = \frac{c}{8\pi}\mathrm{Re}[\vec{E}^*(z)\times\vec{H}(z)] \tag{B2}$$

implying that none of the three Cartesian components of the energy density flux **S** depends on the transverse coordinates x and y. Energy conservation argument implies that the component S_z of the energy flux does not depend on the coordinate z either, while the transverse components S_x and S_y may depend on z. Indeed, in the case of steady-state oscillations in a lossless medium we have, with consideration for Eq. (B2)

$$\nabla \cdot \mathbf{S} = \partial_z S_z(z) = 0,$$

which together with Eq. (B2) gives

$$S_z(\vec{r}) = S_z = \text{const}, \quad S_x(\vec{r}) = S_x(z), \quad S_y(\vec{r}) = S_y(z). \tag{B3}$$

The explicit expression for the z component of the energy flux (B2) is

$$S_z = \frac{1}{2}[E_x^* H_y - E_y^* H_x + E_x H_y^* - E_y H_x^*] = \frac{1}{2}(\Psi, J\Psi). \tag{B4}$$

The tangential components of the energy flux can also be expressed in terms of the column vector $\Psi(z)$ from Eq. (38). Using expressions (40) for E_z and H_z and eliminating these field components from $\mathbf{S}(z)$ in Eq. (B2) yields

$$S_x = \frac{1}{2}(\Psi, \hat{G}_x \Psi), \quad S_y = \frac{1}{2}(\Psi, \hat{G}_y \Psi), \tag{B5}$$

where G_x and G_y are Hermitian matrices,

$$G_x = \begin{bmatrix} 0 & -\frac{n_y}{\mu_{33}} & 0 & \frac{\varepsilon_{13}}{\varepsilon_{33}} \\ -\frac{n_y}{\mu_{33}} & 2\frac{n_x}{\mu_{33}} & -\frac{\mu_{13}^*}{\mu_{33}} & \frac{\varepsilon_{23}}{\varepsilon_{33}} - \frac{\mu_{23}^*}{\mu_{33}} \\ 0 & -\frac{\mu_{13}}{\mu_{33}} & 0 & -\frac{n_y}{\varepsilon_{33}} \\ \frac{\varepsilon_{13}^*}{\varepsilon_{33}} & \frac{\varepsilon_{23}^*}{\varepsilon_{33}} - \frac{\mu_{23}}{\mu_{33}} & -\frac{n_y}{\varepsilon_{33}} & 2\frac{n_x}{\varepsilon_{33}} \end{bmatrix},$$

$$G_y = \begin{bmatrix} 2\frac{n_y}{\mu_{33}} & -\frac{n_x}{\mu_{33}} & -\frac{\varepsilon_{13}}{\varepsilon_{33}} + \frac{\mu_{13}^*}{\mu_{33}} & \frac{\mu_{23}^*}{\mu_{33}} \\ -\frac{n_x}{\mu_{33}} & 0 & -\frac{\varepsilon_{23}}{\varepsilon_{33}} & 0 \\ -\frac{\varepsilon_{13}^*}{\varepsilon_{33}} + \frac{\mu_{13}}{\mu_{33}} & -\frac{\varepsilon_{23}^*}{\varepsilon_{33}} & 2\frac{n_y}{\varepsilon_{33}} & -\frac{n_x}{\varepsilon_{33}} \\ \frac{\mu_{23}}{\mu_{33}} & 0 & -\frac{n_x}{\varepsilon_{33}} & 0 \end{bmatrix}.$$

Both G_x and G_y are functions of the Cartesian coordinate z, frequency ω, and the direction $\vec{n}$ of incident wave propagation.

[1] Pochi Yeh, *Optical Waves in Layered Media* (Wiley, New York, 1988).

[2] Amnon Yariv and Pochi Yeh, *Optical Waves in Crystals: Propagation and Control of Laser Radiation* (Wiley, New York, 1984).

[3] Weng Cho Chew, *Waves and Fields in Inhomogeneous Media* (Van Nostrand Reinhold, New York, 1990).

[4] Y. Fink, J.N. Winn, S. Fan, C. Chen, J. Michel, J.D. Joannopoulos, and E.L. Thomas, Science **282**, 1679 (1998).

[5] J.N. Winn, Y. Fink, S. Fan, and J.D. Joannopoulos, Opt. Lett. **23**, 1573 (1998).

[6] D.N. Chigrin, A.V. Lavrinenko, D.A. Yarotsky, and S.V. Gaponenko, Appl. Phys. A: Mater. Sci. Process. **A68**, 25 (1999).

[7] Ch. Luo, S. Johnson, and J. Joannopoulos, Phys. Rev. B **65**, 201104 (2002).

[8] M. Notomi, Phys. Rev. B **62**, 10696 (2000).

[9] M. Soljacic, S. Johnson, S. Fan, M. Ibanescu, E. Ippen, and J. Joannopoulos, J. Opt. Soc. Am. B **19**, 2052 (2002).

[10] J. Bendickson, J. Dowling, and M. Scalora, Phys. Rev. E **53**, 4107 (1996).

[11] G. D'Aguano *et al.*, Phys. Rev. E **64**, 016609 (2001).

[12] M. Scalora, R.J. Flynn, S.B. Reinhardt, R.L. Fork, M.J. Bloemer, M.D. Tocci, C.M. Bowden, H.S. Ledbetter, J.M. Bendickson, J.P. Dowling, and R.P. Leavitt, Phys. Rev. E **54**, R1078 (1996).

[13] M. Scalora, M.J. Bloemer, A.S. Manka, J.P. Dowling, C.M. Bowden, R. Viswanathan, and J.W. Haus, Phys. Rev. A **56**, 3166 (1997).

[14] A. Mandatori, C. Sibilia, M. Centini, G. D'Aguanno, M. Bertolotti, M. Scalora, M. Bloemer, and C.M. Bowden, J. Opt. Soc. Am. B **20**, 504 (2003).

[15] A. Figotin and I. Vitebsky, Phys. Rev. E **63**, 066609 (2001).

[16] A. Figotin and I. Vitebskiy, Phys. Rev. B **67**, 165210 (2003).

[17] D.W. Berreman, J. Opt. Soc. Am. A **62**, 502 (1972).

[18] I. Abdulhalim, J. Opt. A, Pure Appl. Opt. **2**, 557 (2000).

[19] I. Abdulhalim, J. Opt. A, Pure Appl. Opt. **1**, 646 (1999).

[20] M.G. Krein and V.A. Jacubovich, *Four Papers on Ordinary Differential Equations*, American Mathematical Society Translations, Series 2 (American Mathematical Society, Providence, R.I., 1983), Vol. 120, pp. 1–70.

[21] R. Bellman, *Introduction to Matrix Analysis* (SIAM, Philadelphia, 1997).

[22] E. Coddington and R. Carlson, *Linear Ordinary Differential Equations* (SIAM, Philadelphia, 1997).

[23] All four eigenmodes belong now to the same irreducible representation of the wave vector symmetry group.

[24] M_{11} and M_{22} are also nonzero in the presence of materials with *linear magnetoelectric effect* (see, for example, Ref. [15], and references therein). Usually, this effect is prohibited by symmetry, and we are not considering here such an exotic situation.

[25] In the case of a finite slab, all four eigenmodes (58) would contribute to $\Psi_T(z)$.